

Article

Pretreatment of Biogas Slurry by Modified Biochars to Promote High-Value Treatment of Wastewater by Microalgae

Zhiqiang Gu ¹, Qi Zhang ¹ , Guobi Sun ¹, Jiaxin Lu ^{2,*}, Yuxin Liu ³, Zhenxia Huang ³, Shuming Xu ⁴, Jianghua Xiong ⁵ and Yuhuan Liu ^{1,*}

¹ State Key Laboratory of Food Science and Technology, Engineering Research Center for Biomass Conversion, Nanchang University, Ministry of Education, Nanchang 330047, China

² Key Laboratory of Cleaner Production and Integrated Resource Utilization of China National Light Industry, Beijing Technology and Business University, Beijing 100048, China

³ Jiangxi Rural Energy and Environment Agency, Nanchang 330000, China

⁴ Dingnan Agricultural and Rural Bureau, Ganzhou 341900, China

⁵ Agricultural Ecology and Resources Protection Station of Jiangxi Province, Nanchang 330046, China

* Correspondence: lujiaxin@btbu.edu.cn (J.L.); liuyuhuan@ncu.edu.cn (Y.L.)

Abstract: High concentrations of contaminants such as ammonia nitrogen and organic matter in full-strength wastewater severely inhibit the growth of microalgae, contributing to lower biomass accumulation and contaminant removal efficiency. To overcome this limitation, modified biochars prepared from pine sawdust and sugarcane bagasse were used in this study as an adsorbent–desorbent for the pretreatment of wastewater to promote the growth of microalgae. The results showed that the two modification methods (acid/alkaline modification and magnesium salt modification) used in the experiment could increase the abundance of oxygen-containing functional groups. Moreover, magnesium salt modification could effectively improve the pore structure of biochar surfaces and increase the specific surface areas. Compared with the pristine biochars, the adsorption performance of the modified biochar was found to be significantly higher for nutrients in wastewater. The adsorption capacity of the acid/alkaline-modified pine sawdust biochar reached 8.5 and 16.49 mg·g⁻¹ for ammonia nitrogen and total organic carbon in wastewater, respectively. The magnesium salt modified pine sawdust biochar achieved a more comprehensive nutrients adsorption capacity of 15.68, 14.39, and 3.68 mg·L⁻¹ for ammonia nitrogen, total organic carbon, and total phosphorus, respectively. The mechanism of ammonia nitrogen adsorption was mainly the complexation of surface -OH functional groups, while the adsorption mechanism for phosphate was mainly the complexation of -OH and Mg-O functional groups and the chemical precipitation of MgO or Mg(OH)₂ attached to the surface.

Keywords: biochar; biogas slurry; wastewater pretreatment; modification; nutrients removal



Citation: Gu, Z.; Zhang, Q.; Sun, G.; Lu, J.; Liu, Y.; Huang, Z.; Xu, S.; Xiong, J.; Liu, Y. Pretreatment of Biogas Slurry by Modified Biochars to Promote High-Value Treatment of Wastewater by Microalgae. *Sustainability* **2023**, *15*, 3153. <https://doi.org/10.3390/su15043153>

Academic Editor: Alessio Siciliano

Received: 30 December 2022

Revised: 2 February 2023

Accepted: 6 February 2023

Published: 9 February 2023



Copyright: © 2023 by the authors. Licensee MDPI, Basel, Switzerland. This article is an open access article distributed under the terms and conditions of the Creative Commons Attribution (CC BY) license (<https://creativecommons.org/licenses/by/4.0/>).

1. Introduction

Microalgae is an important biomass resource that can be used to produce animal feed, plant fertilizer, and biodiesel [1], etc., and in some peculiar cases can also be used as a novel biosorbent for the recovery of valuable elements from waste streams [2,3]. However, high cultivation cost is an obstacle to the commercialization of microalgae [4]. In recent years, the use of urban wastewater for microalgae cultivation has been studied as a possible way to reduce the cultivation cost and commercialize microalgal biomass, in some cases resulting in the successful creation of pilot plants [5]. Previous studies reported the use of biogas slurry, municipal sewage, dairy-derived liquid digestate, and many other sources of wastewater for microalgae cultivation [6–8]. Among all of these wastewater sources, in biogas slurry, it was found that microalgae are also able to absorb organic matter, ammonia nitrogen, and phosphorus as nutrients for growth [9]. Indeed, the cultivation of microalgae in biogas slurry can recover nutrients at high efficiency and low cost, realizing the resource utilization of biogas slurry and producing microalgal biomass.

Currently, cultivation of microalgae in full-strength biogas slurry is difficult to achieve because of the high concentration of nutrients. The higher levels of nutrients such as organic matter and $\text{NH}_4^+\text{-N}$ in biogas slurry severely inhibit the growth of microalgae [8]. For example, high concentrations of $\text{NH}_4^+\text{-N}$ in biogas slurry can cause depolarization of the cell membrane of microalgae, leading to inhibition of intracellular anion transport and ultimately disturbing the growth and metabolism of microalgae [10]. The free fatty acids in biogas slurry have cytotoxic effects on the cytoplasmic membrane of some microalgae, causing changes in the permeability of the cytoplasmic membrane, resulting in the leakage of K^+ from the inside of cells and the stress lysis of algal cells [11]. Therefore, it is necessary to pretreat biogas slurry before using it for microalgae cultivation.

Traditionally, common pretreatment methods for biogas slurry include freshwater dilution [12], air-bubbling assisted ammonium stripping [13], and ozone oxidation [14]. Although these methods can reduce the toxicity of biogas slurry to microalgae to some extent, they suffer from high freshwater consumption, limited types of contaminants treated, and high cost, and are not suitable for large-scale pretreatment of biogas slurry.

Adsorption is regarded as an effective wastewater treatment technology because it has the advantage of economical, direct, and effective removal of contaminants [15]. Different adsorbents, such as zeolite [16] and activated carbon [17], have been reported to be effective in adsorbing contaminants from wastewater; however, there are significant limitations of both adsorbents due to the limited availability of zeolite and the high cost of activated carbon [18,19]. Light-weight biochar is a new type of adsorbent that uses various types of waste biomass pyrolyzed under low or no oxygen conditions, including forest residues [20], agricultural residues [21], food processing waste [22], and animal manure [23]. Owing to its high porosity [24], large specific surface areas [25], and large ion exchange capacity [26], biochar is emerging as an environmentally friendly and economical alternative for the removal of inorganic and organic contaminants from the aqueous phase [27]. In recent years, many studies on the use of biochar as an adsorbent have been conducted. Yang et al. [28] prepared biochars from pine sawdust and wheat straw to study their adsorption effects on $\text{NH}_4^+\text{-N}$ and found that the adsorption effect of biochar prepared from pine sawdust on $\text{NH}_4^+\text{-N}$ was higher than that of biochar prepared from wheat straw, and the adsorption mechanism was attributed mainly to electrostatic attraction and chemical bonding. Jiang et al. [29] prepared ZnAl-layered double hydroxide-loaded banana straw biochar (ZnAl-LDH-BSB) through a hydrothermal method to evaluate its adsorption effect on phosphate and found that the largest adsorption of ZnAl-LDH-BSB on phosphate reached $185.19 \text{ mg}\cdot\text{g}^{-1}$. Lima et al. [30] compared the adsorption capacity of biochars from eight different raw materials for Cu^{2+} , Cd^{2+} , Ni^{2+} , and Zn^{2+} before and after modification, and showed that the modified biochar could be a better heavy metal adsorbent because of its higher specific surface areas and more effective functional groups. Chun et al. [31] conducted a study on the adsorption of benzene and nitrobenzene on acid-modified wheat straw biochar at different pyrolysis temperatures and revealed that biochars prepared at high pyrolysis temperature (500–700 °C) had strong surface adsorption due to its higher specific surface areas.

Pine sawdust is a by-product of sawmill sawing, and sugarcane bagasse is a by-product generated in large amounts by sugar and alcohol industries, both of which are often disposed of as waste or simply burned to produce bioenergy. At present, crop straw as a bioenergy has been gradually replaced by new energy sources. The preparation of biochar from pine sawdust and sugarcane bagasse and the use of biochar as an adsorbent to remove contaminants from wastewater could have the dual function of waste utilization and pollution reduction. Biochar is prepared by high-temperature carbonization, which can be used as an adsorbent for nitrogen and phosphorus, so as to realize the reuse of agricultural and forestry wastes, and at the same time, biochar adsorbed with ammonia nitrogen and phosphorus can be returned to the field as a slow-release fertilizer.

In this study, pine sawdust and sugarcane bagasse were used as raw materials to prepare nine biochars by changing the pyrolysis conditions and modification methods for

the removal of nutrients from simulated wastewater. The specific objectives of this study were to: (1) compare and determine the nine biochar adsorption capacities of nutrients; (2) study the possible adsorption mechanisms of nutrients; and (3) provide references for pretreating wastewater and promoting microalgal biomass accumulation.

2. Materials and Methods

2.1. Wastewater Characteristics

In this study, simulated wastewater was prepared based on real biogas slurry characteristics, and the average values of nutrient concentrations in the effluent of a matching anaerobic fermentation project in a pig farm (114.93° E, 27.80° N, Xinyu, China) were referred to determine the concentrations of simulated wastewater indicators (Table 1). Compositions of simulated wastewater were shown as follows: CH₃COONa (0.68 g·L⁻¹), K₂HPO₄ (0.25 g·L⁻¹), KH₂PO₄ (0.25 g·L⁻¹), NH₄Cl (3.60 g·L⁻¹), Yeast Extract Powder (1.00 g·L⁻¹), Peptone (0.50 g·L⁻¹), Na₂CO₃ (1.00 g·L⁻¹). Initial pH value of the simulated wastewater was around 8.65. All chemicals were of analytical grade and purchased from Sinopharm Chemical Reagents Co., Ltd. (121.48° E, 31.23° N, Shanghai, China).

Table 1. Characterization of the sterilized simulated wastewater.

Parameter	Values (Means ± SD)
Total carbon (TC) (mg·L ⁻¹)	953.70 ± 5.14
Total organic carbon (TOC) (mg·L ⁻¹)	877.20 ± 4.80
Inorganic carbon (IC) (mg·L ⁻¹)	76.50 ± 0.34
Total nitrogen (TN) (mg·L ⁻¹)	1198.00 ± 17.00
Ammonia nitrogen (NH ₄ ⁺ -N) (mg·L ⁻¹)	955.00 ± 1.50
Total phosphorus (TP) (mg·L ⁻¹)	150.00 ± 0.60
pH	8.65 ± 0.00

2.2. Preparation and Characterization of Biochars

2.2.1. Preparation of Biochars

In the present study, nine biochars were prepared, characterized, and used for adsorption purposes (four pristine biochars and five modified biochars). Pine sawdust and sugarcane bagasse were selected as raw materials for the present study and they were purchased at a farmer's market (115.96° E, 28.68° N, Nanchang, China). These two raw materials were milled into powders with particle sizes smaller than 0.5 mm. Then, all powdered materials were washed with deionized water (DI, 18.2 MΩ) three times and dried at 80 °C overnight.

First, starting from the raw materials, two pristine biochars were prepared. In order to obtain the optimal adsorption performance, the optimal pyrolysis temperatures for the preparation of pristine biochars from pine sawdust and sugarcane bagasse were referred in Yang et al. [32] and Ding et al. [33], respectively. The pristine pine sawdust biochar (PS300) and pristine sugarcane bagasse biochar (SB400) were produced at the pyrolysis temperatures of 300 °C and 400 °C, respectively, and the pyrolysis reactions were carried out in a tube furnace (OTF-1200X, KEJING, CN) with a residence time of 4 h. The tubular furnace temperature was programmed to increase its temperature by 5 °C·min⁻¹ until it reached the specified value. To ensure uniform heating conditions and an oxygen-free environment, nitrogen (N₂) was used as flush gas. Afterward, it was rinsed 3 times with DI water and dried at 80 °C overnight.

Then, two modification methods were applied (acid/alkaline modification and magnesium salt modification) [21] to the previously prepared pristine biochars and pine sawdust, in order to obtain three modified biochars. First, the two pristine biochars prepared above (PS300 and SB400) were modified by acid/alkaline modification method and prepared two modified biochars (A-PS300 and A-SB400). Briefly, for their preparation, 10 g of each biochar was impregnated in 1 M HCl and 1 M NaOH at a ratio of 10:1 (*v/w*) for 4 h in turn. Then, the biochars were washed to neutral with DI water and dried at 80 °C overnight.

Secondly, the third modified biochar was prepared by applying a magnesium salt modification method to the pine sawdust, also changing the pyrolyzation conditions. In particular, about 40 g of pine sawdust was dipped in 1 M MgCl_2 solution at a mass-to-volume ratio of 1:10 for 2 h [34]; during this period the mixture was shaken several times. After that, the solution was heated until nearly dry and then dried at 80 °C overnight. Finally, the treated samples were pyrolyzed to obtain the modified biochar (Mg-PS500-2.5). In this case, pyrolysis temperature was increased to 500 °C to further increase the BET surface areas of biochar [35]. Moreover, the pyrolysis time was reduced from 4 h to 2.5 h in order to reduce energy consumption and wastewater pretreatment costs.

In addition, in order to compare the effects of different pyrolysis temperatures and pyrolysis times on the adsorption effect of biochar under magnesium salt modification, pine sawdust samples treated with 1 M MgCl_2 solution were pyrolyzed for 4 h at 300 °C and 500 °C (Mg-PS300 and Mg-PS500-4), and two pristine biochars without pretreatment were pyrolyzed at 500 °C for 2.5 h and 4 h (PS500-2.5 and PS500-4). The conditions for preparation were described above. Finally, all biochars were sieved to a mesh size of 0.25–0.28 mm and stored in desiccator for characterization and adsorption experiments.

2.2.2. Characterization of Biochars

The functional groups present in biochars were measured by a Fourier transform infrared (FTIR) spectrometer (Tensor-27, Bruker, DE) in the range of 400 to 4000 cm^{-1} . The surface morphology of biochar samples was examined using a scanning electron microscopy (SEM) system (HITACHI, Regulus 8100, JPN). The surface areas of biochar samples were determined by N_2 adsorption at 77 K on a surface area analyzer (JWGB, JW-BK132F, CN).

2.3. Adsorption and Desorption Experiments

To evaluate the difference in adsorption and desorption capacity of biochars from the two raw materials (pine sawdust and sugarcane bagasse), adsorption and desorption experiments were conducted with the two pristine biochars (PS300 and SB400). Adsorption experiment was conducted at 25 ± 0.5 °C by combining 1.0 g of biochar with 30 mL of sterilized simulated wastewater in a 50 mL centrifuge tube. Tubes were oscillated evenly, then continuously shaken at $120 \text{ r}\cdot\text{min}^{-1}$ at 25 ± 0.5 °C for 72 h. During this time, the concentrations of NH_4^+ -N, TN, TOC, IC, TC, and TP were determined by taking 1 mL of sample solution at 3, 6, 12, 24, 48, and 72 h. Before each sampling, the water sample was allowed to stand for 10 min before the supernatant was taken. The supernatant was filtered with a 0.45 μm membrane filter in order to recover only the liquid phase. Then, the filtrate was diluted: (i) 10 times for TC, IC, TOC, and TN analysis, which were performed using a TOC/TN analyzer (Multi N/C 3100, Analytik Jena AG, Germany); and (ii) 200 times for NH_4^+ -N and TP analysis using a multiparameter water quality analyzer (5B–6C, Lianhua, China). In the desorption experiment, the biochars (PS300 and SB400) were taken out at the end of the adsorption experiment and then dried naturally. The collected biochars were added to a 50 mL centrifuge tube with 30 mL sterilized DI water and then continuously shaken at $120 \text{ r}\cdot\text{min}^{-1}$ at 25 ± 0.5 °C for 72 h. The concentrations of NH_4^+ -N, TN, TOC, IC, TC, and TP were determined in the supernatant with the same sampling times and methodology described above for the adsorption experiment.

Then, the equilibrium adsorption capacities of five modified biochars (A-PS300, A-SB400, Mg-PS300, Mg-PS500-2.5, and Mg-PS500-4) and a pristine biochar (PS500-2.5) were determined. Adsorption experiment was conducted at 25 °C by combining 1.0 g of biochar with 30 mL of sterilized simulated wastewater in a 50 mL centrifuge tube. The tube was oscillated evenly, then put in the constant temperature shaker ($120 \text{ r}\cdot\text{min}^{-1}$). The above adsorption experiment proved that 24 h reaction time was sufficient to ensure that the six biochars reached adsorption saturation. So, 24 h later, the sample solution was filtered through with a 0.45 μm membrane filter, and then the concentrations of NH_4^+ -N, TN, TOC, IC, TC, and TP were determined. Measurement methods were as described earlier.

All above experiments were set up in three replicates and the average values were calculated. The amount of $\text{NH}_4^+\text{-N}$, TN, TOC, IC, TC, and TP adsorption at reaction equilibrium was calculated according to Equation:

$$q_e = \frac{V(C_0 - C_e)}{m}$$

where q_e is the adsorption capacity of biochar (mg g^{-1}), C_0 and C_e are the initial and equilibrium concentrations ($\text{mg}\cdot\text{L}^{-1}$), respectively, V is the volume of the sterilized simulated wastewater (L), and m is the mass of the biochar (g).

3. Results and Discussion

3.1. Characterization of Biochars

Figure 1 shows the SEM images of PS300 (a), A-PS300 (b), SB400 (c), A-SB400 (d), Mg-PS300 (e), and Mg-PS500-2.5 (f). The six biochars differed greatly in microscopic morphology due to different types of raw materials, pyrolysis conditions, and modification methods. Figure 1 shows that the surface of PS300 was rough and showed an irregular pore structure with a certain number of honeycomb pores, suggesting that it facilitated the capacitation of old and new pores during the activation process. It was also observed that many particles were deposited on the surface of PS300 and no pore structure was found in the larger protrusions compared to PS500 (Figure S1), suggesting that the pyrolysis of biomass at low temperatures was not sufficient and the pores had not been opened. Compared with PS300, the pore volumes and average pore diameters of A-PS300 increased. This was due to the strong etching effect of alkali liquor on biochars during the chemical modification process, which would clear the blockages in the pore structure and open up the internal pore channels of biochars to form micropores [36]. As shown in Figure 1e and f, the Mg-PS300 and Mg-PS500-2.5 surfaces were loose and porous with abundant honeycomb pores. This might be because the addition of MgCl_2 changed the pore structure of the biochar surface and promoted the generation of new pores [37]. In addition, since the pyrolysis temperature of Mg-PS500-2.5 was higher than that of Mg-PS300, this could translate into a higher release of volatile substances and the formation of new pores [38]. At the same time, it was found that when magnesium-modified biochar was prepared under pyrolysis conditions at $500\text{ }^\circ\text{C}$, the number of honeycomb pores on the surface of biochar decreased with the extension of pyrolysis time (from 2.5 h to 4 h) (Figure S2).

The surface of SB400 was relatively smooth, with a tight texture and no obvious pores (Figure 1). No noticeable difference was detected between SB400 and A-SB400, which might be due to the relatively smooth surface and denser texture of SB400, resulting in a less effective acid and alkaline treatment.

The BET surface areas of PS300, A-PS300, SB400, A-SB400, and Mg-PS500-2.5 are given in Table 2. There was a significant increase in the BET surface areas of the Mg-PS500-2.5 ($243.60\text{ m}^2\cdot\text{g}^{-1}$). Ling et al. [39] also found a similar increase in the BET surface areas of MgO nanoparticles embedded in nitrogen self-doped hydrophyte derived biochar compared to the pristine nitrogen self-doped hydrophyte derived biochar. Zhang et al. [37] discovered that MgO particles are polycrystalline and highly porous with a pore size of 2–4 nm, so this morphology would result in higher BET surface areas for MgO-modified biochar.

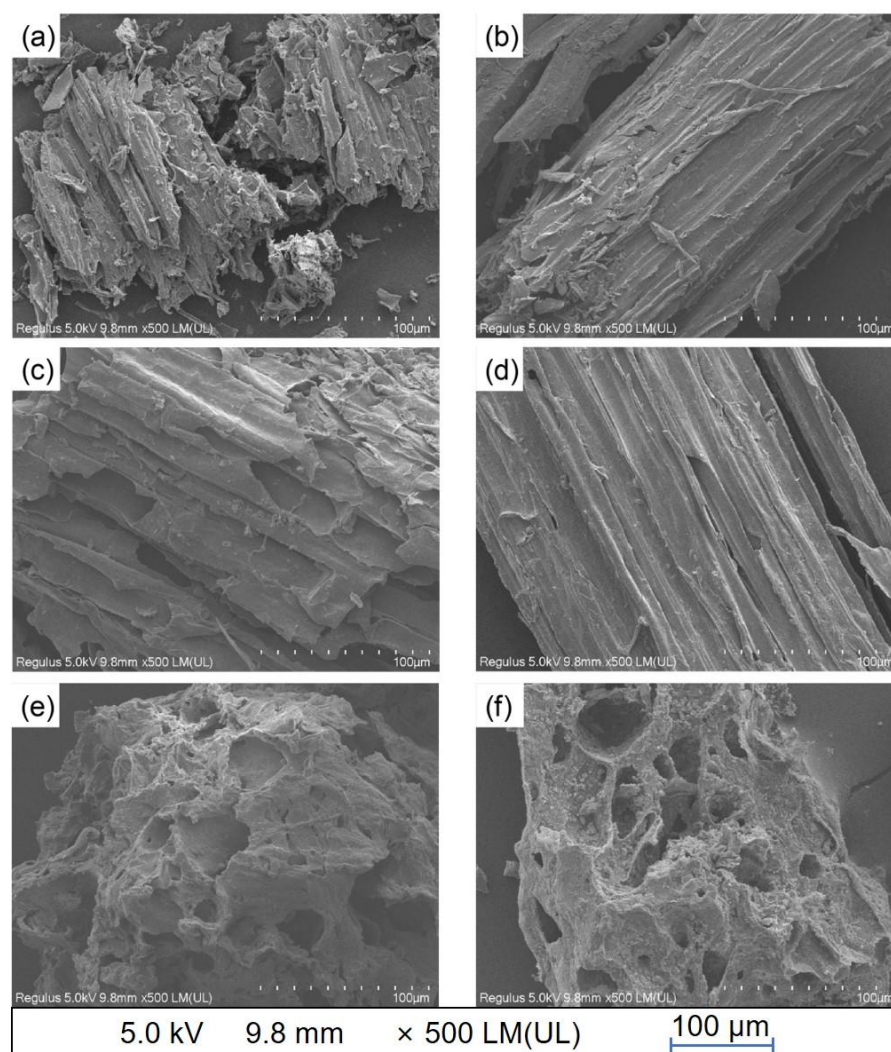


Figure 1. SEM images of the five biochars: (a) PS300, (b) A-PS300, (c) SB400, (d) A-SB400, (e) Mg-PS300, and (f) Mg-PS500-2.5.

Table 2. The BET surface areas of PS300, A-PS300, SB400, A-SB400, and Mg-PS500-2.5.

Sample Code	BET Surface Areas ($\text{m}^2 \cdot \text{g}^{-1}$)
PS300	1.77
A-PS300	2.20
SB400	5.05
A-SB400	3.36
Mg-PS500-2.5	243.60

The FTIR spectrum, shown in Figure 2, was performed to identify the main functional groups in biochars. According to the infrared spectrum, the band at around 3420 cm^{-1} represents -OH, which is mainly related to the hydrogen bond stretching vibration of water molecules [40], and the stretching vibration of C=O and -C-O lie at 1617 cm^{-1} and 1263 cm^{-1} , respectively, suggesting that the surfaces of the five biochars were rich in oxygen-containing functional groups. The oxygen atoms in these functional groups and the hydrogen atoms in the amino groups can attract each other to form stable hydrogen bonds, which have a superior NH_4^+ -N adsorption effect [41]. Notably, the Mg-PS500-2.5 showed an agglomerate-OH stretching vibrational band at a wave number of 3700 cm^{-1} , which indicated that more -OH was generated after the magnesium salt modification [42].

While the Mg-O absorption vibrational band appeared at 567 cm^{-1} [28], Mg-O is an active functional group that can combine with PO_4^{3-} -P to form Mg-O-P complexes.

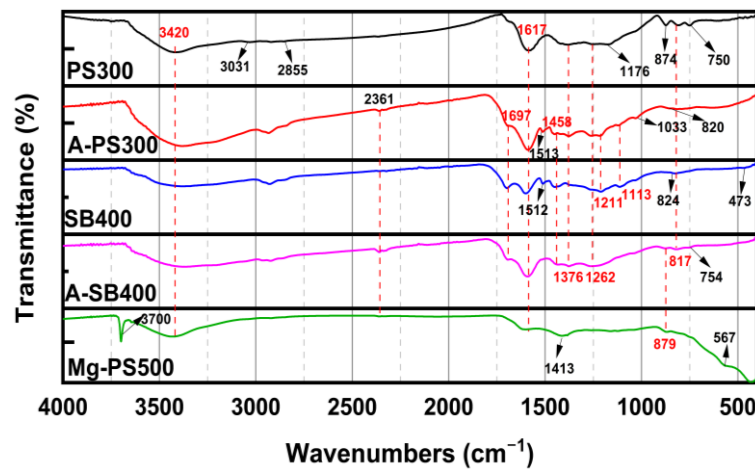


Figure 2. FTIR spectra: PS300, A-PS300, SB400, A-SB400, and Mg-PS500-2.5.

3.2. Performance of Raw Materials on Adsorption and Desorption

The physical and chemical surface properties of biochar depend on many factors, including raw material type, pyrolysis conditions, and pyrolysis methods [43]. Aiming to investigate the type of raw materials for nutrient removal, the adsorption of nutrients from wastewater by two pristine biochars (PS300 and SB500) prepared from pine sawdust and sugarcane bagasse is given in Figure 3.

It can be clearly seen that the adsorption of both biochars for contaminants, except for total phosphorus, reached equilibrium after 24 h. Interestingly, the adsorption capacities of PS300 and SB400 for inorganic carbon were -3.05 and $-2.22\text{ mg}\cdot\text{g}^{-1}$, respectively, suggesting that both biochars released inorganic carbon into the water during the treatment of wastewater, which might be caused by the release of the carbonate formed during the pyrolysis of biochar into wastewater. The carbonate released into the water could be used as a source of inorganics and supplied to microalgae for photosynthesis, thus promoting the growth of microalgae. It can be clearly seen that PS300 had better adsorption performance than SB400 for nutrients. The adsorption capacity of the PS300 for NH_4^+ -N was $2.26\text{ mg}\cdot\text{g}^{-1}$, which was significantly higher than that of SB400 ($1.12\text{ mg}\cdot\text{g}^{-1}$) ($p < 0.05$). Combined with the BET surface area characterization results, although the BET surface area of PS300 was smaller than that of SB400, the adsorption performance for nutrients was better, which suggested that the adsorption performance of biochars was not only determined by the specific surface areas. FTIR characterization results showed that both PS300 and SB400 were rich in oxygen-containing functional groups such as -OH, C=O, and -C-O, which may be involved in the adsorption of contaminants in wastewater. For example, Guo et al. [44] found that the adsorption of NH_4^+ -N by biochar was related to C=O, and the presence of C=O on the biochar surface could improve its adsorption capacity for NH_4^+ -N. Lou et al. [45] found that the increase in oxygen-containing functional groups (-OH and C=O) on the surface of biochar interacted with polar ammonium nitrate in solution to form ionic bonds, which increased the equilibrium adsorption of NH_4^+ -N by biochar. The content of -OH and C=O in PS300 was found to be higher than that of SB400 by FTIR spectrum, which may be the main reason for the higher adsorption capacity of PS300 on NH_4^+ -N than that of SB400. Although the two pristine biochar (PS300 and SB400) had considerable adsorption effects on organic carbon (9.00 and $6.11\text{ mg}\cdot\text{g}^{-1}$, respectively), they had poor adsorption effects on NH_4^+ -N and phosphorus, with the adsorption capacities of TP being only 0.35 and $0.26\text{ mg}\cdot\text{g}^{-1}$. This was mainly due to the usually negatively charged surface of pristine biochars and the lack of metal cations, resulting in its limited adsorption capacity for phosphate [46,47].

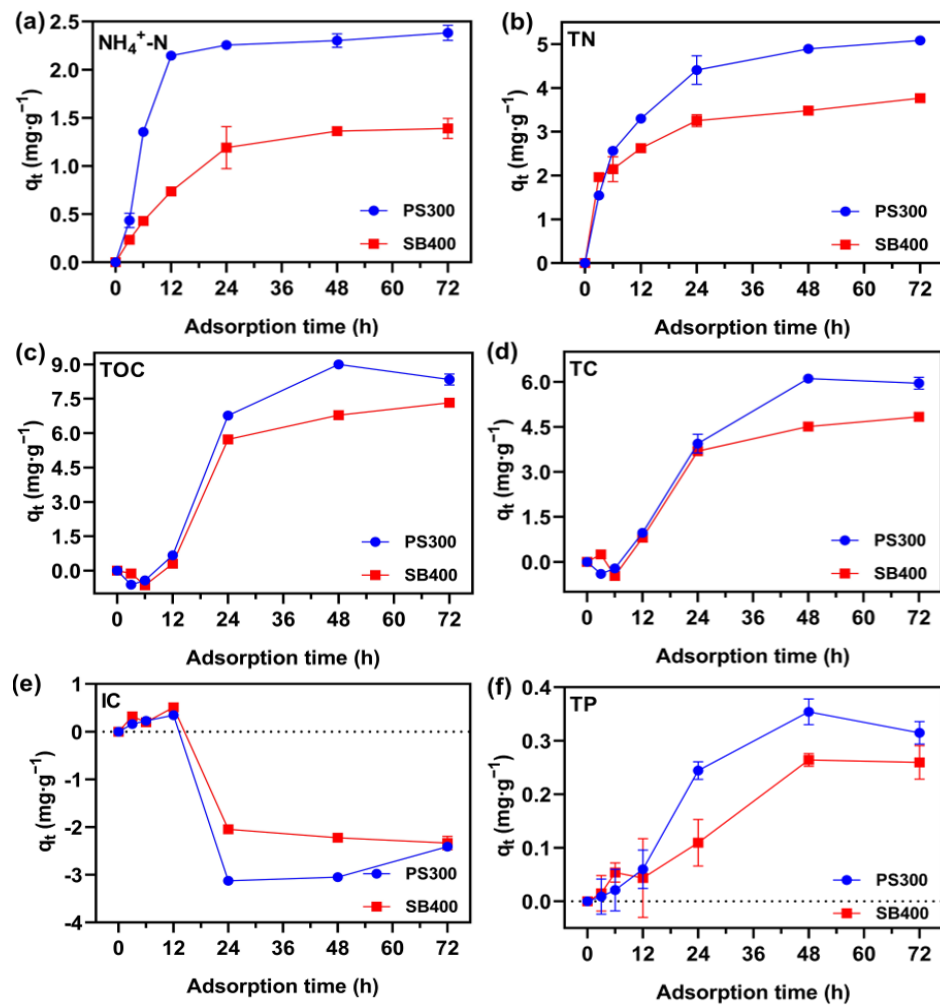


Figure 3. Effect of raw material types on nutrients adsorption of two pristine biochars (PS300 and SB400) (q_t represents t hours of adsorption after the amount of nutrient adsorbed at the time of adsorption): (a) $\text{NH}_4^+\text{-N}$, (b) TN, (c) TOC, (d) TC, (e) IC, and (f) TP.

The potential of PS300 and SB400 to desorb nutrients into DI water is presented in Figure 4. Driven by the ion concentration gradient, PS300 and SB400 were able to slowly release nutrients such as $\text{NH}_4^+\text{-N}$, inorganic carbon, and $\text{PO}_4^{3-}\text{-P}$ back into water and reached equilibrium after about 12 h [48]. The desorption capacities of the two biochars were approximately equivalent. Cai et al. [49] found that $\text{NH}_4^+\text{-N}$ was the preferred nitrogen source for the growth of microalgae and when the concentration was too low, it limited the growth of microalgae. The results showed that PS300 and SB400 would release the adsorbed $\text{NH}_4^+\text{-N}$ back into an aqueous phase when the $\text{NH}_4^+\text{-N}$ concentration in the aqueous phase was low, maintaining the $\text{NH}_4^+\text{-N}$ concentration at a relatively stable level. More importantly, the ratio of $\text{NH}_4^+\text{-N}$ to TP released into the aqueous phase by PS300 and SB400 remained in the range of 9.9–18.2:1 during 12–72 h, and the N/P ratio in this range was suitable for the growth of microalgae [50].

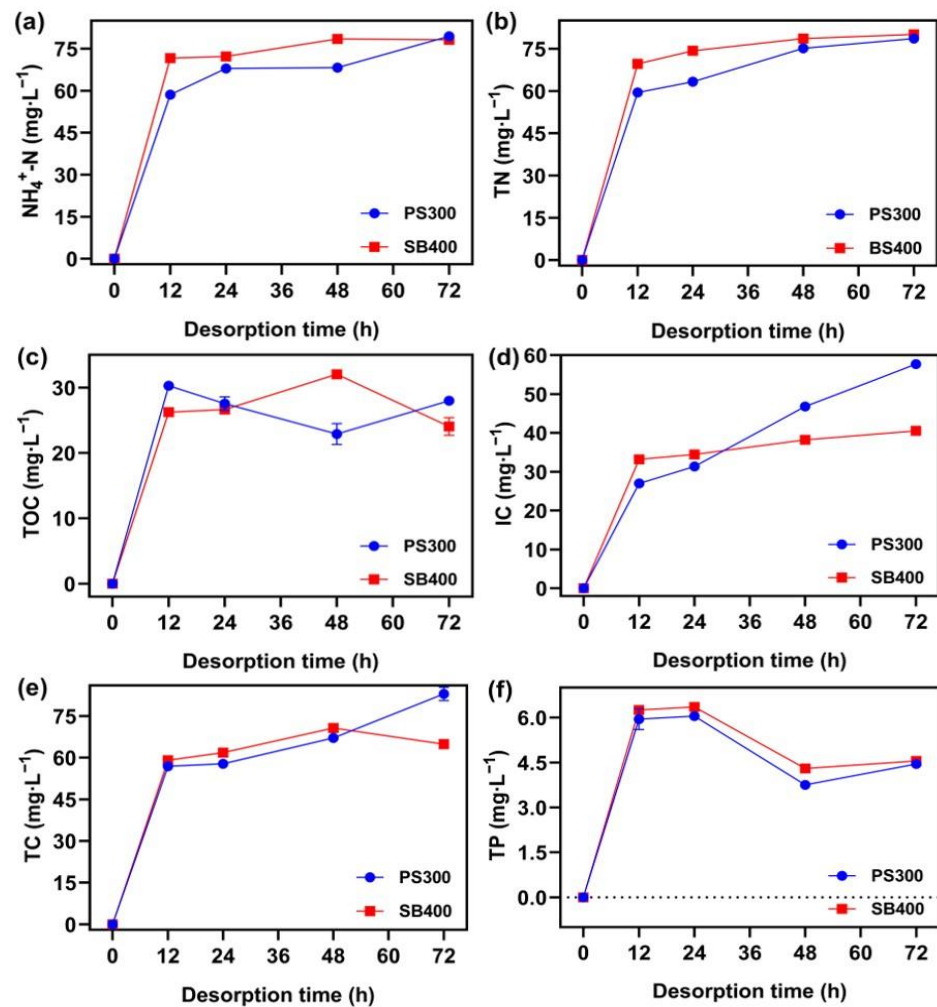


Figure 4. Effect of raw material types on nutrients desorption of two pristine biochars (PS300 and SB400): (a) NH_4^+ -N, (b) TN, (c) TOC, (d) TC, (e) IC, and (f) TP.

In conclusion, it took about 24 and 12 h for the two pristine biochars to reach adsorption equilibrium, respectively. In terms of the adsorption effect, it was more suitable to choose pine sawdust as raw material to prepare biochar for the pretreatment of biogas slurry. However, due to the limitation of its own characteristics such as small specific surface areas and underdeveloped pores, the adsorption capacity of pristine biochar was limited, and it needed to be modified to change its physical and chemical properties to increase its adsorption capacity for more efficient pretreatment of biogas slurry.

3.3. Effect of Modification of Biochars on Wastewater Adsorption Performances

3.3.1. Acid/Alkaline Modification

Modification can improve the physical and chemical properties of biochar, such as specific surface areas and pore structure, or introduce various functional groups on the surface of biochar, which in turn improves the adsorption performance of biochar [51]. First, the adsorption performance of two acid/alkaline modified biochars (A-PS300 and A-SB400) was evaluated. As can be seen in Figure 5, the adsorption capacities of A-PS300 for NH_4^+ -N, TN, TOC, TC, and TP were 8.5, 13.45, 16.49, 11.43, and 0.88 $\text{mg}\cdot\text{g}^{-1}$, respectively, which were increased by 270%, 175%, 83%, 87%, and 151%, respectively, compared with PS300. The adsorption capacities of A-SB400 for NH_4^+ -N, TN, TOC, TC, and TP were 4.44, 9.18, 16.98, 11.75, and 0.73 $\text{mg}\cdot\text{g}^{-1}$, respectively, which were 226%, 164%, 150%, 161%, and 181% higher than those of SB400. In conclusion, the adsorption capacities of the acid/alkaline

modified biochars (A-PS300 and A-SB400) were significantly higher ($p < 0.05$) for various nutrients in wastewater compared to the pristine biochars (PS300 and SB400).

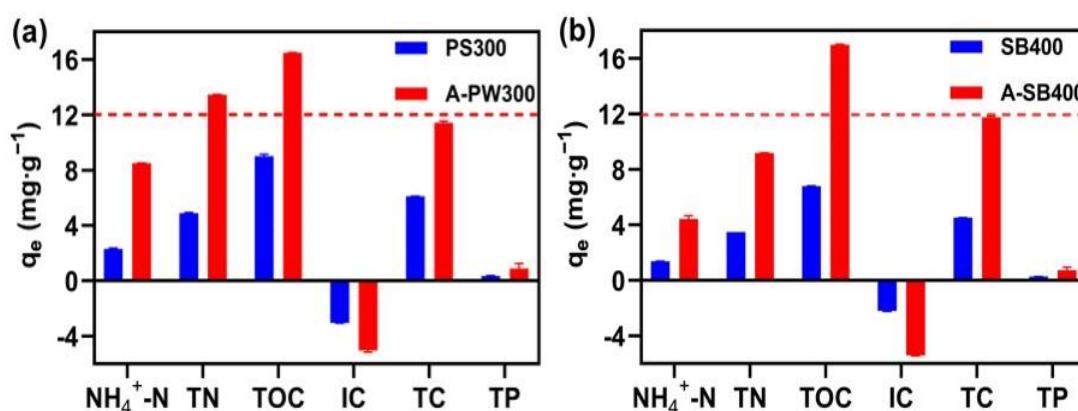


Figure 5. Removal of nutrients from wastewater by pristine biochars (PS300 and SB400) and acid/alkaline modified biochars (A-PS300 and A-SB400): (a) PS biochars, and (b) SB biochars.

The phosphorus adsorption capacity of A-PS300 and A-SB400, although significantly improved, was still not satisfactory. This might be because the acid/alkaline modification did not change the nature of the charge on the surface of the biochar, and the negative charge on the surface of the biochar prevented its adsorption of phosphorus. The acid/alkaline modified biochars showed the most significant improvement in the adsorption performance of NH₄⁺-N. The BET and SEM characterization results showed that the BET surface areas of A-PS300 and A-SB400 did not change significantly after modification. Therefore, the improvement in adsorption performance might be mainly caused by the change in surface functional groups after acid/alkaline modification [52]. It was found by FTIR spectrum that the bonds O-H at 3420 cm⁻¹ and C=O at 1617 cm⁻¹ were increased in A-PS300 and A-SB400, and the presence of O-H and C=O could enhance the NH₄⁺-N adsorption capacity of biochar [44]. Kastner et al. [53] confirmed that treatment of biochar with dilute sulfuric acid and ozone could remove non-NH₃ ions loaded on acidic functional groups on the surface of biochar, thus providing more adsorption sites for NH₃ ion adsorption and greatly improving the adsorption capacity of biochar for NH₃. Liu et al. [54] also found that modifying bio-tea biochar with NaOH solution could increase the number of acidic functional groups on the surface of biochar, leading to an increase in its NH₄⁺-N adsorption capacity.

3.3.2. Magnesium Salt Modification

The adsorption of nutrients in wastewater by A-PS300 and A-SB400 was improved to some extent by acid/alkaline modification but the adsorption capacity of both was extremely limited for anions (e.g., Phosphate). Takaya et al. [55] found that the mineral composition of the biochar itself plays a larger important role in phosphate adsorption than the surface areas available for adsorption. Moreover, we found that the acid/alkaline modification did not improve the physical and chemical properties of biochar very well through the previous experiment. To further improve the adsorption effect of biochar, pine sawdust was selected as the raw material for magnesium salt modification. Modification with MgCl₂ was performed to reduce the surface electronegativity and improve the adsorption capacity of biochar for anions.

The adsorption of nutrients from wastewater by magnesium salt modified biochars is given in Table 3. It can be seen from the table that for the two pristine biochars (PS300 and PS500-2.5), PS300 was ideal for the adsorption of various nutrients in wastewater overall, which was consistent with the results reported by Yang et al. [32]. Compared with the two pristine biochars (PS300 and PS500-2.5), it was found that the magnesium salt modified biochars (Mg-PS300 and Mg-PS500-2.5) obtained under the same preparation conditions

had a significant improvement in the adsorption effect of $\text{NH}_4^+\text{-N}$ and TP. It was worth noting that the adsorption capacity of biochar for organic matter after magnesium salt modification at 300 °C was negative. This might be because the presence of magnesium salts led to insufficient pyrolysis of biochar and some organic carbon still remained. Compared with the three magnesium salt modified biochars, the adsorption effect of biochar on the nutrients in wastewater was the most ideal for pyrolysis for 2.5 h at 500 °C. Notably, the adsorption capacities of Mg-PS500-2.5 reached 15.68 and 3.68 $\text{mg}\cdot\text{g}^{-1}$ for $\text{NH}_4^+\text{-N}$ and TP, respectively, which were significantly higher than those of Mg-PS300 (6.20 and 2.91 $\text{mg}\cdot\text{g}^{-1}$) ($p < 0.05$). At the same time, it was found that with the increase in pyrolysis time (2.5 h to 4 h) at 500 °C, it was found that the adsorption capacity of magnesium salt modified biochar on each nutrient in wastewater decreased, which may be related to the increase in pyrolysis time, resulting in a decrease in the number of honeycomb pores on the surface of biochar (Figure S2). The adsorption capacity of Mg-PS500-2.5 for $\text{NH}_4^+\text{-N}$ was 15.68 $\text{mg}\cdot\text{g}^{-1}$, higher than those of many other adsorbents (Table 4). For example, biochar produced from oak sawdust through the participation of Lanthanum (La) only exhibited a maximum $\text{NH}_4^+\text{-N}$ adsorption capacity of 7.86 $\text{mg}\cdot\text{g}^{-1}$ [56]. This result might be attributed to the higher BET surface areas of Mg-PS500-2.5 (243.60 $\text{m}^2\cdot\text{g}^{-1}$). The correlation analysis showed that the adsorption capacities of $\text{NH}_4^+\text{-N}$ and TP were related to the specific surface areas of biochar, and the larger the specific surface areas, the more significant the adsorption effect [57]. However, combined with the previous findings, it was speculated that the specific surface area was not the main factor affecting the adsorption capacity of biochar for $\text{NH}_4^+\text{-N}$ and TP. Instead, it was more likely caused by the changes in oxygen-containing functional groups on the surface of biochar. According to the FTIR spectrum, Mg-PS500-2.5 showed an agglomerate-OH stretching vibration peak at 3700 cm^{-1} , indicating that acid or alcohols were more abundant and could increase the adsorption of $\text{NH}_4^+\text{-N}$ and phosphate through functional group interaction [41]. Moreover, the Mg-O absorption peak appeared at 567 cm^{-1} , where Mg-O could combine with $\text{PO}_4^{3-}\text{-P}$ to form Mg-O-P complexes, thus promoting the adsorption of phosphate. Zhang et al. [13] also found that the wave peaks of the -OH bond at 3669 cm^{-1} and the Mg-O bond at 553 cm^{-1} of the MgO-modified biochar almost disappeared after the adsorption of nitrogen and phosphorus, indicating that they were both involved in the reaction of adsorbed nitrogen and phosphorus. Finally, the MgO or $\text{Mg}(\text{OH})_2$ attached to the surface of Mg-PS500-2.5 might react with phosphate to form a complex containing magnesium and phosphorus. Fang et al. [58] found the presence of a considerable number of nanoparticles in the mesoporous structures of magnesium-loaded biochar (nano-MgO particles), and the adsorption effect mainly relied on the chemical actions of nano-MgO particles.

Table 3. The adsorption capacities of nutrients from wastewater of PS300, Mg-PS300, PS500-2.5 h, Mg-PS500-2.5, and Mg-PS500-4.

q_e ($\text{mg}\cdot\text{g}^{-1}$)	PS300	Mg-PS300	PS500-2.5	Mg-PS500-2.5	Mg-PS500-4
$\text{NH}_4^+\text{-N}$	2.30 ± 0.07	6.20 ± 0.58	3.22 ± 0.45	15.68 ± 0.34	6.98 ± 0.68
TN	4.89 ± 0.06	8.63 ± 0.21	0.82 ± 0.15	23.18 ± 0.49	4.34 ± 0.44
TOC	9.00 ± 0.16	−4.94 ± 0.59	3.13 ± 0.35	14.39 ± 0.15	0.97 ± 0.12
IC	−3.05 ± 0.01	−7.82 ± 0.86	−2.38 ± 0.28	1.32 ± 0.05	−2.50 ± 0.47
TC	6.11 ± 0.01	−12.76 ± 0.39	0.75 ± 0.12	13.28 ± 0.02	−1.10 ± 0.54
TP	0.35 ± 0.02	2.91 ± 0.01	0.35 ± 0.03	3.68 ± 0.01	2.92 ± 0.02

Table 4. Biochars applied for removal of $\text{NH}_4^+\text{-N}$ from wastewater.

Adsorbent	Treatment Temperature	Adsorption Capacity (mg g^{-1})	Reference
Oak sawdust	300 °C	3.12	[56]
Oak sawdust impregnated with LaCl_3	300 °C	7.86	[56]
Pine sawdust	300 °C	5.38	[32]
Mixed hardwood	300 °C	2.80	[59]
Pineapple peel	400 °C	13.40	[60]
Magnetic steel slag	500 °C	4.36	[61]
Giant reed	500 °C	1.49	[62]
Sludge residue	600 °C	9.85	[63]
Corn cob	600 °C	1.09	[64]
Sorghum distillers grain	750 °C	14.34	[65]

In summary, compared with acid/alkaline modified biochars and pristine biochars, magnesium salt modification could significantly improve the adsorption of $\text{NH}_4^+\text{-N}$ and phosphate, which determines that magnesium salt modified biochar might be more suitable for the pretreatment of biogas slurry.

4. Conclusions

This study revealed that the adsorption of nutrients from wastewater by biochar was related to the selected raw material, and the adsorption capacity of the pristine biochar for nutrients was lower than the results achieved with modified biochar. It showed that both pristine biochars could release nutrients to the aqueous phase in reverse at low nutrient concentrations in wastewater, and the ratio of released $\text{NH}_4^+\text{-N}$ to $\text{PO}_4^{3-}\text{-P}$ was suitable for the growth of microalgae. Acid/alkaline modification could increase the content of -OH and C=O on the surface of biochar, thus promoting the adsorption of $\text{NH}_4^+\text{-N}$ through the complexation of -OH and C=O . Compared with acid/alkaline modification, the magnesium salt modification made the biochar surface rich in -OH functionality; moreover, it could significantly improve the pore structure of the biochar surface and increase the specific surface areas. Finally, the presence of Mg^{2+} reduced the negative charge density on the biochar surface, thus decreasing the electrostatic repulsion of phosphate. The adsorption of $\text{NH}_4^+\text{-N}$ by magnesium salt modified biochar mainly depended on the complexation of -OH functional groups on its surface. The phosphate adsorption on the one hand benefited from the reduction in the negative charge density on the surface of biochar, and on the other hand depended on the complexation of -OH and Mg-O functional groups and the chemical precipitation of MgO or Mg(OH)_2 attached to the surface. Although the tests were conducted on simulated wastewater, the results suggest that pine sawdust biochar modified with magnesium salt is a valuable adsorbent for nutrients in biogas slurry. Its use in the pre-treatment of wastewater could concretely help with reducing the presence of toxic compounds that may negatively impact the growth of microalgae in the effluent, encouraging the realization of a system for the simultaneous production of microalgae biomass and wastewater treatment.

Supplementary Materials: The following supporting information can be downloaded at: <https://www.mdpi.com/article/10.3390/su15043153/s1>, Figure S1: SEM images of the PS300 and PS500-4 (100 μm); Figure S2: SEM images of the Mg-PS500-2.5 and Mg-PS500-4 (100 μm).

Author Contributions: Conceptualization, Z.G. and Q.Z.; methodology, Z.G. and Y.L. (Yuhuan Liu); data curation, Z.G. and G.S.; formal analysis, Z.G., Q.Z., G.S., J.L. and Y.L. (Yuxin Liu); writing original draft, Z.G. and Q.Z.; writing review and editing, J.L. and Y.L. (Yuhuan Liu); visualization, Z.H., S.X. and J.X.; funding acquisition, Q.Z. and J.L. All authors have read and agreed to the published version of the manuscript.

Funding: This research was funded by the Open Research Fund Program of the Key Laboratory of Cleaner Production and Integrated Resource Utilization of China's National Light Industry, grant number CP2021YB07; the National Natural Science Foundation of China, grant number 22106062; and the Natural Science Foundation of Jiangxi Province, grant number 20212BAB214063.

Institutional Review Board Statement: Not applicable.

Informed Consent Statement: Not applicable.

Data Availability Statement: Not applicable.

Conflicts of Interest: The authors declare no conflict of interest.

References

1. Katiyar, R.; Gurjar, B.R.; Biswas, S.; Pruthi, V.; Kumar, N.; Kumar, P. Microalgae: An emerging source of energy based bio-products and a solution for environmental issues. *Renew. Sustain. Energy Rev.* **2017**, *72*, 1083–1093. [[CrossRef](#)]
2. Sirakov, M.; Palmieri, M.; Iovinella, M.; Davis, S.J.; Petriccione, M.; di Cicco, M.R.; De Stefano, M.; Ciniglia, C. Cyanidiophyceae (Rhodophyta) Tolerance to Precious Metals: Metabolic Response to Palladium and Gold. *Plants* **2021**, *10*, 2367. [[CrossRef](#)] [[PubMed](#)]
3. Iovinella, M.; Lombardo, F.; Ciniglia, C.; Palmieri, M.; di Cicco, M.R.; Trifuoggi, M.; Race, M.; Manfredi, C.; Lubritto, C.; Fabbicino, M.; et al. Bioremoval of Yttrium (III), Cerium (III), Europium (III), and Terbium (III) from Single and Quaternary Aqueous Solutions Using the Extremophile *Galdieria sulphuraria* (Galdieriaceae, Rhodophyta). *Plants* **2022**, *11*, 1376. [[CrossRef](#)] [[PubMed](#)]
4. Tan, X.-B.; Zhao, X.-C.; Yang, L.-B.; Liao, J.-Y.; Zhou, Y.-Y. Enhanced biomass and lipid production for cultivating *Chlorella pyrenoidosa* in anaerobically digested starch wastewater using various carbon sources and up-scaling culture outdoors. *Biochem. Eng. J.* **2018**, *135*, 105–114. [[CrossRef](#)]
5. di Cicco, M.R.; Iovinella, M.; Palmieri, M.; Lubritto, C.; Ciniglia, C. Extremophilic Microalgae *Galdieria* Gen. for Urban Wastewater Treatment: Current State, the Case of "POWER" System, and Future Prospects. *Plants* **2021**, *10*, 2343. [[CrossRef](#)]
6. Zhu, S.; Feng, S.; Xu, Z.; Qin, L.; Shang, C.; Feng, P.; Wang, Z.; Yuan, Z. Cultivation of *Chlorella vulgaris* on unsterilized dairy-derived liquid digestate for simultaneous biofuels feedstock production and pollutant removal. *Bioresour. Technol.* **2019**, *285*, 121353. [[CrossRef](#)]
7. Abeysiriwardana-Arachchige, I.S.A.; Munasinghe-Arachchige, S.P.; Delanka-Pedige, H.M.K.; Nirmalakhandan, N. Removal and recovery of nutrients from municipal sewage: Algal vs. conventional approaches. *Water Res.* **2020**, *175*, 115709. [[CrossRef](#)]
8. Gu, Z.; Liu, Y.; Zou, G.; Zhang, Q.; Lu, R.; Yan, H.; Cao, L.; Liu, T.; Ruan, R. Enhancement of nutrients removal and biomass accumulation of *Chlorella vulgaris* in pig manure anaerobic digestate effluent by the pretreatment of indigenous bacteria. *Bioresour. Technol.* **2021**, *328*, 124846. [[CrossRef](#)]
9. Zhang, H.; Gong, W.; Zeng, W.; Yan, Z.; Jia, B.; Li, G.; Liang, H. Organic carbon promotes algae proliferation in membrane-aeration based bacteria-algae symbiosis system (MA-BA). *Water Res.* **2020**, *176*, 115736. [[CrossRef](#)]
10. Ritchie, R.J. The Ammonia Transport, Retention and Futile Cycling Problem in Cyanobacteria. *Microb. Ecol.* **2013**, *65*, 180–196. [[CrossRef](#)]
11. Wu, J.-T.; Chiang, Y.-R.; Huang, W.-Y.; Jane, W.-N. Cytotoxic effects of free fatty acids on phytoplankton algae and cyanobacteria. *Aquat. Toxicol.* **2006**, *80*, 338–345. [[CrossRef](#)]
12. Marchão, L.; da Silva, T.L.; Gouveia, L.; Reis, A. Microalgae-mediated brewery wastewater treatment: Effect of dilution rate on nutrient removal rates, biomass biochemical composition, and cell physiology. *J. Appl. Phycol.* **2018**, *30*, 1583–1595. [[CrossRef](#)]
13. Zhang, L.; Lee, Y.-W.; Jahng, D. Ammonia stripping for enhanced biomethanization of piggery wastewater. *J. Hazard. Mater.* **2012**, *199*, 36–42. [[CrossRef](#)]
14. Lu, Q.; Han, P.; Chen, F.; Liu, T.; Li, J.; Leng, L.; Li, J.; Zhou, W. A novel approach of using zeolite for ammonium toxicity mitigation and value-added *Spirulina* cultivation in wastewater. *Bioresour. Technol.* **2019**, *280*, 127–135. [[CrossRef](#)]
15. Rajapaksha, A.U.; Chen, S.S.; Tsang, D.C.; Zhang, M.; Vithanage, M.; Mandal, S.; Gao, B.; Bolan, N.S.; Ok, Y.S. Engineered/designer biochar for contaminant removal/immobilization from soil and water: Potential and implication of biochar modification. *Chemosphere* **2016**, *148*, 276–291. [[CrossRef](#)]
16. de Magalhães, L.F.; da Silva, G.R.; Peres, A.E.C. Zeolite Application in Wastewater Treatment. *Adsorpt. Sci. Technol.* **2022**, *2022*, 4544104. [[CrossRef](#)]
17. Ramutshatsha-Makhwedzha, D.; Mavhungu, A.; Moropeng, M.L.; Mbaya, R. Activated carbon derived from waste orange and lemon peels for the adsorption of methyl orange and methylene blue dyes from wastewater. *Heliyon* **2022**, *8*, e09930. [[CrossRef](#)]
18. Ahmad, M.; Lee, S.S.; Dou, X.M.; Mohan, D.; Sung, J.-K.; Yang, J.E.; Ok, Y.S. Effects of pyrolysis temperature on soybean stover- and peanut shell-derived biochar properties and TCE adsorption in water. *Bioresour. Technol.* **2012**, *118*, 536–544. [[CrossRef](#)]
19. Wang, S.; Peng, Y. Natural zeolites as effective adsorbents in water and wastewater treatment. *Chem. Eng. J.* **2010**, *156*, 11–24. [[CrossRef](#)]
20. Aghababaei, A.; Ncibi, M.C.; Sillanpää, M. Optimized removal of oxytetracycline and cadmium from contaminated waters using chemically-activated and pyrolyzed biochars from forest and wood-processing residues. *Bioresour. Technol.* **2017**, *239*, 28–36. [[CrossRef](#)]

21. Georgieva, V.G.; Gonsalves, L.; Tavlieva, M.P. Thermodynamics and kinetics of the removal of nickel (II) ions from aqueous solutions by biochar adsorbent made from agro-waste walnut shells. *J. Mol. Liq.* **2020**, *312*, 112788. [[CrossRef](#)]
22. de Jesus, J.H.F.; Matos, T.T.D.S.; Cunha, G.D.C.; Mangrich, A.S.; Romão, L.P.C. Adsorption of aromatic compounds by biochar: Influence of the type of tropical biomass precursor. *Cellulose* **2019**, *26*, 4291–4299. [[CrossRef](#)]
23. Thang, P.Q.; Jitae, K.; Giang, B.L.; Viet, N.; Huong, P.T. Potential application of chicken manure biochar towards toxic phenol and 2,4-dinitrophenol in wastewaters. *J. Environ. Manag.* **2019**, *251*, 109556. [[CrossRef](#)] [[PubMed](#)]
24. Sanchez-Monedero, M.A.; Cayuela, M.L.; Roig, A.; Jindo, K.; Mondini, C.; Bolan, N.J.B.T. Role of biochar as an additive in organic waste composting. *Bioresour. Technol.* **2018**, *247*, 1155–1164. [[CrossRef](#)]
25. Zhu, Q.; Wu, J.; Wang, L.; Yang, G.; Zhang, X. Adsorption Characteristics of Pb²⁺ onto Wine Lees-Derived Biochar. *Bull. Environ. Contam. Toxicol.* **2016**, *97*, 294–299. [[CrossRef](#)]
26. Mosa, A.; El-Ghamry, A.; Tolba, M. Functionalized biochar derived from heavy metal rich feedstock: Phosphate recovery and reusing the exhausted biochar as an enriched soil amendment. *Chemosphere* **2018**, *198*, 351–363. [[CrossRef](#)]
27. Oliveira, F.R.; Patel, A.K.; Jaisi, D.P.; Adhikari, S.; Lu, H.; Khanal, S.K. Environmental application of biochar: Current status and perspectives. *Bioresour. Technol.* **2017**, *246*, 110–122. [[CrossRef](#)]
28. Yang, Q.; Wang, X.; Luo, W.; Sun, J.; Xu, Q.; Chen, F.; Zhao, J.; Wang, S.; Yao, F.; Wang, D.; et al. Effectiveness and mechanisms of phosphate adsorption on iron-modified biochars derived from waste activated sludge. *Bioresour. Technol.* **2018**, *247*, 537–544. [[CrossRef](#)]
29. Jiang, Y.-H.; Li, A.-Y.; Deng, H.; Ye, C.-H.; Li, Y. Phosphate adsorption from wastewater using ZnAl-LDO-loaded modified banana straw biochar. *Environ. Sci. Pollut. Res.* **2019**, *26*, 18343–18353. [[CrossRef](#)]
30. Lima, I.M.; Boateng, A.A.; Klasson, K.T. Physicochemical and adsorptive properties of fast-pyrolysis bio-chars and their steam activated counterparts. *J. Chem. Technol. Biotechnol.* **2010**, *85*, 1515–1521. [[CrossRef](#)]
31. Chun, Y.; Sheng, G.; Chiou, C.T.; Xing, B. Compositions and Sorptive Properties of Crop Residue-Derived Chars. *Environ. Sci. Technol.* **2004**, *38*, 4649–4655. [[CrossRef](#)]
32. Yang, H.I.; Lou, K.; Rajapaksha, A.U.; Ok, Y.S.; Anyia, A.O.; Chang, S.X. Adsorption of ammonium in aqueous solutions by pine sawdust and wheat straw biochars. *Environ. Sci. Pollut. Res.* **2018**, *25*, 25638–25647. [[CrossRef](#)]
33. Ding, W.; Dong, X.; Ime, I.M.; Gao, B.; Ma, L.Q. Pyrolytic temperatures impact lead sorption mechanisms by bagasse biochars. *Chemosphere* **2014**, *105*, 68–74. [[CrossRef](#)]
34. Jiang, Y.-H.; Li, A.-Y.; Deng, H.; Ye, C.-H.; Wu, Y.-Q.; Linmu, Y.-D.; Hang, H.-L. Characteristics of nitrogen and phosphorus adsorption by Mg-loaded biochar from different feedstocks. *Bioresour. Technol.* **2019**, *276*, 183–189. [[CrossRef](#)]
35. Zhao, S.-X.; Ta, N.; Wang, X.-D. Effect of Temperature on the Structural and Physicochemical Properties of Biochar with Apple Tree Branches as Feedstock Material. *Energies* **2017**, *10*, 1293. [[CrossRef](#)]
36. Jin, H.; Hanif, M.U.; Capareda, S.; Chang, Z.; Huang, H.; Ai, Y. Copper(II) removal potential from aqueous solution by pyrolysis biochar derived from anaerobically digested algae-dairy-manure and effect of KOH activation. *J. Environ. Chem. Eng.* **2016**, *4*, 365–372. [[CrossRef](#)]
37. Zhang, M.; Gao, B.; Yao, Y.; Xue, Y.; Inyang, M. Synthesis of porous MgO-biochar nanocomposites for removal of phosphate and nitrate from aqueous solutions. *Chem. Eng. J.* **2012**, *210*, 26–32. [[CrossRef](#)]
38. Suliman, W.; Harsh, J.B.; Abu-Lail, N.I.; Fortuna, A.-M.; Dallmeyer, I.; Garcia-Perez, M. Influence of feedstock source and pyrolysis temperature on biochar bulk and surface properties. *Biomass Bioenergy* **2016**, *84*, 37–48. [[CrossRef](#)]
39. Ling, L.-L.; Liu, W.-J.; Zhang, S.; Jiang, H. Magnesium Oxide Embedded Nitrogen Self-Doped Biochar Composites: Fast and High-Efficiency Adsorption of Heavy Metals in an Aqueous Solution. *Environ. Sci. Technol.* **2017**, *51*, 10081–10089. [[CrossRef](#)]
40. Hodúr, C.; Bellahsen, N.; Mikó, E.; Nagypál, V.; Šreš, Z.; Kertész, S. The Adsorption of Ammonium Nitrogen from Milking Parlor Wastewater Using Pomegranate Peel Powder for Sustainable Water, Resources, and Waste Management. *Sustainability* **2020**, *12*, 4880. [[CrossRef](#)]
41. Meng, Y.; Wang, Y.; Wang, C. Phosphorus Release and Adsorption Properties of Polyurethane–Biochar Crosslinked Material as a Filter Additive in Bioretention Systems. *Polymers* **2021**, *13*, 283. [[CrossRef](#)] [[PubMed](#)]
42. Vu, T.M.; Trinh, V.T.; Doan, D.P.; Van, H.T.; Nguyen, T.V.; Vigneswaran, S.; Ngo, H.H. Removing ammonium from water using modified corncob-biochar. *Sci. Total Environ.* **2017**, *579*, 612–619. [[CrossRef](#)] [[PubMed](#)]
43. Tan, X.; Liu, Y.; Zeng, G.; Wang, X.; Hu, X.; Gu, Y.; Yang, Z. Application of biochar for the removal of pollutants from aqueous solutions. *Chemosphere* **2015**, *125*, 70–85. [[CrossRef](#)] [[PubMed](#)]
44. Guo, R.; Li, X.; Christie, P.; Chen, Q.; Jiang, R.; Zhang, F. Influence of root zone nitrogen management and a summer catch crop on cucumber yield and soil mineral nitrogen dynamics in intensive production systems. *Plant Soil* **2008**, *313*, 55–70. [[CrossRef](#)]
45. Lou, L.; Luo, L.; Wang, L.; Cheng, G.; Xu, X.; Hou, J.; Xun, B.; Hu, B.; Chen, Y. The influence of acid demineralization on surface characteristics of black carbon and its sorption for pentachlorophenol. *J. Colloid Interface Sci.* **2011**, *361*, 226–231. [[CrossRef](#)]
46. Wang, Z.; Shen, D.; Shen, F.; Li, T. Phosphate adsorption on lanthanum loaded biochar. *Chemosphere* **2016**, *150*, 1–7. [[CrossRef](#)]
47. Li, R.; Wang, J.J.; Zhou, B.; Awasthi, M.K.; Ali, A.; Zhang, Z.; Gaston, L.A.; Lahori, A.H.; Mahar, A. Enhancing phosphate adsorption by Mg/Al layered double hydroxide functionalized biochar with different Mg/Al ratios. *Sci. Total Environ.* **2016**, *559*, 121–129. [[CrossRef](#)]
48. Lin, L.; Lei, Z.; Wang, L.; Liu, X.; Zhang, Y.; Wan, C.; Lee, D.-J.; Tay, J.H. Adsorption mechanisms of high-levels of ammonium onto natural and NaCl-modified zeolites. *Sep. Purif. Technol.* **2013**, *103*, 15–20. [[CrossRef](#)]

49. Cai, T.; Park, S.Y.; Li, Y. Nutrient recovery from wastewater streams by microalgae: Status and prospects. *Renew. Sustain. Energy Rev.* **2013**, *19*, 360–369. [[CrossRef](#)]
50. Choi, H.J.; Lee, S.M. Effect of the N/P ratio on biomass productivity and nutrient removal from municipal wastewater. *Bioprocess Biosyst. Eng.* **2015**, *38*, 761–766. [[CrossRef](#)]
51. da Silva Medeiros, D.C.C.; Nzediegwu, C.; Benally, C.; Messele, S.A.; Kwak, J.-H.; Naeth, M.A.; Ok, Y.S.; Chang, S.X.; El-Din, M.G. Pristine and engineered biochar for the removal of contaminants co-existing in several types of industrial wastewaters: A critical review. *Sci. Total Environ.* **2022**, *809*, 151120. [[CrossRef](#)]
52. Ghorbani, M.; Konvalina, P.; Kopecký, M.; Kolář, L. A meta-analysis on the impacts of different oxidation methods on the surface area properties of biochar. *Land Degrad. Dev.* **2022**, *34*, 299–312. [[CrossRef](#)]
53. Kastner, J.R.; Miller, J.; Das, K.C. Pyrolysis conditions and ozone oxidation effects on ammonia adsorption in biomass generated chars. *J. Hazard. Mater.* **2009**, *164*, 1420–1427. [[CrossRef](#)]
54. Liu, H.; Dong, Y.; Liu, Y.; Wang, H. Screening of novel low-cost adsorbents from agricultural residues to remove ammonia nitrogen from aqueous solution. *J. Hazard. Mater.* **2010**, *178*, 1132–1136. [[CrossRef](#)]
55. Takaya, C.A.; Fletcher, L.A.; Singh, S.; Okwuosa, U.; Ross, A. Recovery of phosphate with chemically modified biochars. *J. Environ. Chem. Eng.* **2016**, *4*, 1156–1165. [[CrossRef](#)]
56. Wang, Z.; Guo, H.; Shen, F.; Yang, G.; Zhang, Y.; Zeng, Y.; Wang, L.; Xiao, H.; Deng, S. Biochar produced from oak sawdust by Lanthanum (La)-involved pyrolysis for adsorption of ammonium (NH₄⁺), nitrate (NO₃⁻), and phosphate (PO₄³⁻). *Chemosphere* **2015**, *119*, 646–653. [[CrossRef](#)]
57. Chu, G.; Zhao, J.; Huang, Y.; Zhou, D.; Liu, Y.; Wu, M.; Peng, H.; Zhao, Q.; Pan, B.; Steinberg, C.E. Phosphoric acid pretreatment enhances the specific surface areas of biochars by generation of micropores. *Environ. Pollut.* **2018**, *240*, 1–9. [[CrossRef](#)]
58. Fang, C.; Zhang, T.; Li, P.; Jiang, R.; Wu, S.; Nie, H.; Wang, Y. Phosphorus recovery from biogas fermentation liquid by Ca–Mg loaded biochar. *J. Environ. Sci.* **2015**, *29*, 106–114. [[CrossRef](#)]
59. Sarkhot, D.V.; Ghezzehei, T.A.; Berhe, A.A. Effectiveness of Biochar for Sorption of Ammonium and Phosphate from Dairy Effluent. *J. Environ. Qual.* **2013**, *42*, 1545–1554. [[CrossRef](#)]
60. Otieno, A.O.; Home, P.G.; Raude, J.M.; Murunga, S.I.; Ngumba, E.; Ojwang, D.O.; Tuhkanen, T. Pineapple peel biochar and lateritic soil as adsorbents for recovery of ammonium nitrogen from human urine. *J. Environ. Manag.* **2021**, *293*, 112794. [[CrossRef](#)]
61. Kim, G.; Kim, Y.M.; Kim, S.M.; Cho, H.; Park, J. Magnetic Steel Slag Biochar for Ammonium Nitrogen Removal from Aqueous Solution. *Energies* **2021**, *14*, 2682. [[CrossRef](#)]
62. Hou, J.; Huang, L.; Yang, Z.; Zhao, Y.; Deng, C.; Chen, Y.; Li, X. Adsorption of ammonium on biochar prepared from giant reed. *Environ. Sci. Pollut. Res.* **2016**, *23*, 19107–19115. [[CrossRef](#)] [[PubMed](#)]
63. Zhang, L.; Deng, F.; Liu, Z.; Ai, L. Removal of ammonia nitrogen and phosphorus by biochar prepared from sludge residue after rusty scrap iron and reduced iron powder enhanced fermentation. *J. Environ. Manag.* **2021**, *282*, 111970. [[CrossRef](#)] [[PubMed](#)]
64. Zhang, Y.; Feng, Y.; Yu, Q.; Xu, Z.; Quan, X. Enhanced high-solids anaerobic digestion of waste activated sludge by the addition of scrap iron. *Bioresour. Technol.* **2014**, *159*, 297–304. [[CrossRef](#)]
65. Hsu, D.; Lu, C.; Pang, T.; Wang, Y.; Wang, G. Adsorption of Ammonium Nitrogen from Aqueous Solution on Chemically Activated Biochar Prepared from Sorghum Distillers Grain. *Appl. Sci.* **2019**, *9*, 5249. [[CrossRef](#)]

Disclaimer/Publisher’s Note: The statements, opinions and data contained in all publications are solely those of the individual author(s) and contributor(s) and not of MDPI and/or the editor(s). MDPI and/or the editor(s) disclaim responsibility for any injury to people or property resulting from any ideas, methods, instructions or products referred to in the content.